Mechanical properties at room temperature of an Al–Zn–Mg–Cu alloy processed by equal channel angular pressing

C.M. Cepeda-Jiménez*, J.M. García-Infanta, O.A. Ruano, F. Carreño

Department of Physical Metallurgy, CENIM, CSIC, Av. Gregorio del Amo 8, 28040 Madrid, Spain

ARTICLE INFO

ABSTRACT

Tensile tests were conducted to evaluate the influence of equal-channel angular pressing (ECAP) on the mechanical properties at room temperature of overaged Al 7075-O alloy. ECAP processing was performed using route B_C at different temperatures and number of passes, i.e. different processing severity conditions. The maximum load (F_{max}) recorded during the last pass of each ECAP path considered in this study is a very good estimation of the processing severity. The mechanical properties were studied in terms of the balance between tensile strength and ductility. In the processed Al 7075-O alloy, the grain size was reduced down to ∼150 nm. Consequently, tensile testing at room temperature revealed a significant increase in the maximum tensile strength after ECAP with respect to the as start material. In the present study, as the processing severity increases with the number of ECAP passes or with the decrease in processing temperature, there is a consistent trend of increment in ultimate tensile strength with minor decrease in uniform plastic elongation respect to the first ECAP pass at room temperature. This is in contrast to the behaviour after more severe plastic deformation conditions, where an increase in strength together with a strong decrease in elongation would be expected.

© 2011 Elsevier B.V. All rights reserved.

1. Introduction

High strength aluminium alloys, such as the Al 7075-T6 alloy, possess a high strength-to-weight ratio, being widely applied in the aerospace industry and in structural engineering. There is nevertheless much interest in further improving the mechanical behaviour of these engineering materials in terms of two parameters, strength and ductility [1–4].

Ultrafine-grained (UFG) and nanostructured metals and alloys acquire very high strength, in accordance with the Hall–Petch relationship [5], but relatively low tensile ductility at ambient temperature [6]. Accordingly, the tensile engineering stress–strain curve peaks at a small plastic strain and then drops precipitously as strain localization occurs, leading to failure [7–10]. This low ductility is attributed to insufficient strain hardening due to an inability to accumulate dislocations [11,12].

Equal-channel angular pressing (ECAP) is a severe plastic deformation method to enhance the strength of metallic alloys through (sub)grain refinement, improving mechanical behaviour with higher strength and good ductility [13,14]. This processing introduces intensive plastic strain into materials through repetitive pressing [15–18].

In general, the microstructure of the ECAPed materials shows a non-equilibrium condition characterized by a high dislocation density and a large number of low angle (sub)grain boundaries [19,20]. This microstructure determines the mechanical properties at room temperature of the processed material.

Age-hardenable alloys are generally difficult to process by equal-channel angular pressing (ECAP) at room temperature because they invariably fail by catastrophic cracking or segmentation [21]. Strong precipitation hardening due to fine precipitation, for example produced by natural ageing of initially solutionised materials, leads to extensive cracking during ECAP processing itself [21,22].

There are few works about the improvement in mechanical properties of the Al 7075 alloy processed by ECAP. Zhao and coworkers [23,24] processed Al 7075 samples in solid solution by ECAP-route B_C at room temperature. After processing, natural ageing for one month was performed. For these processing conditions, the sample strength increased ∼25% till a maximum tensile strength of 720 MPa. However, only two ECAP passes could be performed due to the significant increase in strength due to precipitation of Guinier–Preston zones and η' phase inside the grains.

In the present study, the ECAP processing was conducted on Al 7075 in the overaged condition to facilitate the passing through the ECAP die, and to introduce large accumulative strains. This will allow studying the influence of the processing variables on the mechanical properties. Additionally, it is our contention that the presence of overaged second-phase particles favours the structural

* Corresponding author. Tel.: +34 91 5538900x217; fax: +34 91 5347425.
E-mail address: cm.cepeda@cenim.csic.es (C.M. Cepeda-Jiménez).

Table 1
Chemical composition of the as-received Al 7075 alloy (wt%).

Si	Fe	Zn	Mg	Cu	Cr	Mn	Ti	Al
0.052	0.19	5.68	2.51	1.59	0.19	0.007	0.025	balance

stability at high temperatures after severe deformation processing, of considerable importance for retaining high strength and superplastic characteristics [25,26]. Finally, the strength of the as-received Al 7075 alloy may be essentially restored by conducting an appropriate ageing treatment after forming of the final product.

Therefore, the mechanical properties at room temperature of the overaged Al 7075-O alloy processed by different number of ECAP passes and processing temperatures, i.e. different processing severity, are compared in terms of the balance between strength and tensile elongation, and the results will be discussed and related to the microstructure.

2. Experimental procedure

The aluminium alloy used in the present study was a rolled Al 7075-T651 plate of 12 mm in thickness. The composition in atomic percentage of the alloy is included in Table 1.

As-received Al 7075-T651 samples were subjected to overaging heat treatment at 280 °C during 5 h prior to the ECAP processing to obtain an stable microstructure and to minimize dynamic processes, such as nucleation and precipitates coarsening during ECAP processing.

The nomenclature used for the as start overaged Al 7075 alloy, Al 7075-O, and ECAP processed samples is given in Table 2.

ECAP billets with dimensions 70 mm × 10 mm × 10 mm were machined along the rolling direction of the as-received plate. ECAP processing was performed using a sharp-cornered 90° ECAP die (zero die-relief angle at the outer corner of the die channel intersection), at a pressing speed of 5 mm/min. Fig. 1 shows the reference axes used in this work, where z is the flow plane (FP) normal, y the top plane (TP) normal and x is the cross-section plane (CP) normal. The sense of shear on the shear plane is indicated at the die channel intersection. Samples were ECAP processed by route B_C, i.e. rotated 90° in the same sense between each pass (Fig. 1). This route was selected because it is the optimum processing procedure for attaining an array of equiaxed grains separated by high misorientation angles [27].

The influence of the number of passes and processing temperature has been considered. Each sample was initially pressed once at room temperature ($N_p = 1$), and then pressed repetitively through totals of 3, 5 and 8 passes at 130 °C, equivalent to imposed strains of ~3, 5 and 8, respectively. In addition, samples were ECAP processed through 3 passes at different temperatures of 80, 130 and 180 °C to eval-

Table 2
Nomenclature used for the as start Al 7075 alloy and ECAP processed samples. F_{max} corresponds to the maximum load recorded during the last pass of each ECAP processing path, and it is a proper estimation of the processing severity.

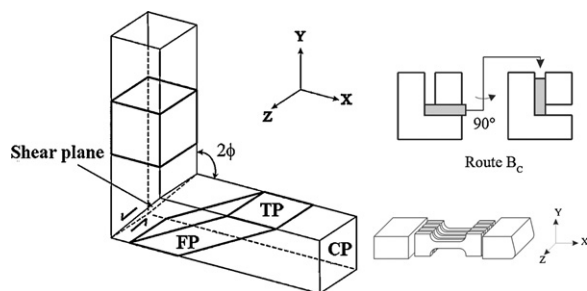| Processing	Nomenclature	F_{max} (kN)
Al 7075-T651 + overaging during 5 h at 280 °C	Al 7075-O	–
1 pass at room temperature (T_{RT})	1p T_{RT}	70 ± 2
1 pass at T_{RT} + 2 passes at 130 °C	3p 130 °C	71 ± 1
1 pass at T_{RT} + 4 passes at 130 °C	5p 130 °C	75 ± 1
1 pass at T_{RT} + 7 passes at 130 °C	8p 130 °C	84 ± 2
1 pass at T_{RT} + 2 passes at 80 °C	3p 80 °C	79 ± 2
1 pass at T_{RT} + 2 passes at 180 °C	3p 180 °C	50 ± 2

Fig. 1. Scheme of the ECAP processing by route B_C. The tensile samples were machined with the tensile axis parallel to the extrusion direction (X).

uate the influence of processing temperature (T_p). More than 3 passes at 80 °C were not possible to achieve because visible cracks appeared on the sample surface. Nor more passes than 3 were performed at 180 °C, since considerable grain coarsening was observed.

The microstructure of processed samples was analyzed by transmission electron microscopy (TEM) using a JEOL JEM 2000 FX II equipment operating at 200 kV. ECAPed samples were always examined at the centre of the flow plane in order to avoid die wall effects. Grain size was measured, for all the processed conditions, from TEM images using the mean linear intercept method, without discriminating between high- and low-angle boundaries, using the Sigma Scan Pro software. More than 300 grains for each processing condition were analyzed. Grain size data fell into log-normal distributions, so the geometric mean value was chosen as a measure of the size.

The misorientation distribution of the ECAP processed samples was obtained with an automated crystallographic orientation mapping (ACOM) tool attached to a JEOL 3010 TEM operating at 300 kV and equipped with a LaB_6 filament. This technique consists in the analysis of spot diffraction patterns and allows to characterize deformed microstructures with (sub)grain size smaller than 100 nm and misorientation ≥1°. However, in this study the misorientation distribution and the fraction of high-angle boundaries (f_{HAB}) were calculated from misorientation data higher than 2°. Thus, a low-angle grain boundary (LAB) was defined by a misorientation between adjacent grains of 2° < θ < 15°, and a high-angle grain boundary (HAB) was defined by θ > 15°. More details about this technique are found elsewhere [28–30].

Monotonic tensile tests were performed to characterize the mechanical properties of the processed Al 7075-O alloy, using a universal hydraulic Instron 1362 testing machine at room temperature with a constant strain rate of 10^{-3} s^{-1}. Planar dog-bone tensile samples of 10 mm × 3 mm × 1.5 mm gage dimensions with a radius of 3 mm were machined out of the ECAP samples parallel to the flow plane (FP), in such a way that the gage length coincided with the middle region of the ECAP samples (Fig. 1), and with the tensile axis parallel to the extrusion direction (X). Tensile samples were also machined from the as start Al 7075-O plate, being parallel to the longitudinal–transversal plane and with the tensile axis parallel to the as-received rolling direction.

3. Results

Table 2 includes the maximum load (F_{max}) recorded by the test machine during the last pass of each ECAP processing path considered in this study. This F_{max} is a very good estimation of the processing severity. It can be observed that F_{max} increases with N_p and decreases with T_p. It is worth noting that F_{max} values corresponding to the last ECAP pass after the processing paths 3p-80 °C and 8p-130 °C are very similar, being 79 and 84 kN, respectively.

Fig. 2 shows TEM micrographs corresponding to the flow plane of ECAP processed Al 7075-O samples after one pass at room temperature (Fig. 2a) and as a function of the number of passes (N_p) at 130 °C (Fig. 2b–d), and the processing temperature (T_p) (Fig. 2e–f). Additionally, Table 3 includes average values of the (sub)grain size (L_Y) for the overaged Al 7075-O alloy, and after different ECAP processing. L_Y corresponds to the shortest length of the (sub)grain microstructure, which in general consists of bands of elongated (sub)grains, approximately aligned in the shear direction.

The as start Al 7075-O alloy after the overaging treatment showed large grains that were elongated and flattened parallel to the rolling direction. The average grain thickness and length in the rolling direction (RD) were about 15 and 350 μm, respectively. After one pass (Fig. 2a), a high density of dislocations is retained and the grain boundaries are wavy and ill-defined. The use of the room temperature for the first pass suppresses dynamic recovery, allowing the density of the accumulated dislocations to reach a higher level than that achievable at higher temperature.

Furthermore, it can be observed that the (sub)grain size decreases with N_p from $L_Y > 400$ nm for one pass at room temperature to $L_Y \sim 163$ nm for the sample processed by eight passes at 130 °C (Fig. 2d and Table 3). A nearly equiaxed (sub)grain structure after eight ECAP passes (Fig. 2d) has replaced the bandlike substructure formed in the initial pressing operation, although a tendency for the (sub)grains to align in the shear direction of the final pressing pass can still be observed. Additionally, there was generally a lower density of intragranular dislocations with an increase in the number of ECAP passes (N_p) (Fig. 2d). In addition, the (sub)grain microstruc-

a) 1p T_{RT}

b) 3p 130ºC
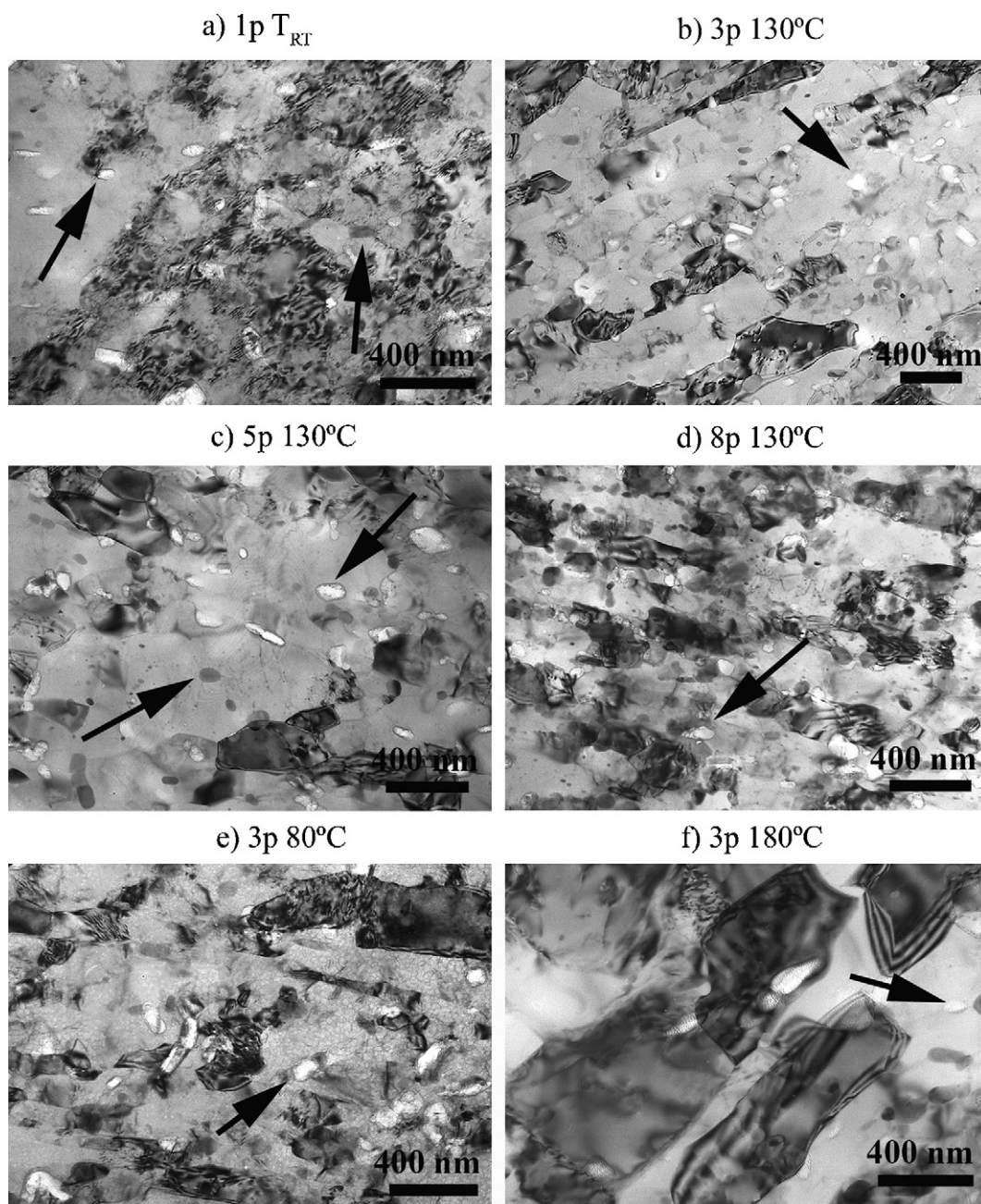
c) 5p 130ºC

d) 8p 130ºC

e) 3p 80ºC

f) 3p 180ºC

Fig. 2. TEM micrographs showing the microstructure of the Al 7075-O alloy after ECAP processing as a function of the number of passes and processing temperature: (a) 1p-T_{RT}; (b) 3p-130 °C; (c) 5p-130 °C; (d) 8p-130 °C; (e) 3p-80 °C and (f) 3p-180 °C.

ture for the Al 7075-O samples processed by 3 ECAP passes as a function of the processing temperature (T_p = 80, 130 and 180 °C), showed also a morphology of elongated (sub)grains in the shear direction (Fig. 2b, e and f, respectively). The (sub)grain size (L_Y) (Table 3) is reduced from L_Y >400 nm in the Al 7075-O processed by 1 ECAP pass (Fig. 2a) to 153 nm in the Al 7075-O alloy processed by 3p at 80 °C (Fig. 2e and Table 3). The microstructure achieved after 3p-80 °C (Fig. 2e) is a typical heavily deformed microstructure with high density of dislocations in nanoscale networks. Fig. 2f shows some microstructure changes when the ECAP processing is performed at higher temperature. The dislocation density within the cells obviously diminished as compared to those formed at lower temperature, and more defined cell boundaries were formed. The mean (sub)grain size increases with the processing temperature up to 180 °C, being $L_Y \sim 318$ nm (Fig. 2f and Table 3). Thus, the most

Table 3
(Sub)grain size (L_Y) measurements (nm) and mechanical properties obtained by tensile tests at room temperature of the as start Al 7075-O alloy and after ECAP processing. s = engineering stress; e_u = uniform plastic elongation; e_F = elongation at fracture.

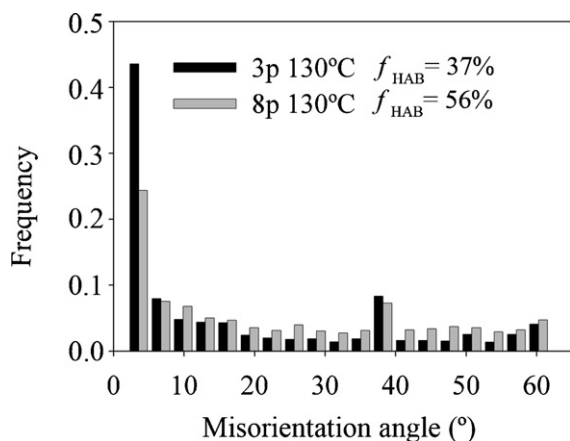| Processing	L_Y (nm)	$s_{0.2}$ (MPa)	s_{max} (MPa)	e_u (%)	e_F (%)
Al 7075-O	~15,000	155	284	9.8 ± 1.4	26
1p T_{RT}	>400	325	357	3.1 ± 0.5	10
3p 130 °C	200 ± 5	320	369	4.8 ± 0.7	13
5p 130 °C	175 ± 6	364	407	3.3 ± 0.6	11
8p 130 °C	163 ± 5	399	442	2.4 ± 0.5	9
3p 80 °C	153 ± 5	392	431	2.4 ± 0.5	5
3p 180 °C	318 ± 17	215	295	8.8 ± 1.2	20

Fig. 3. Misorientation distribution (2–60°) of adjacent grains obtained by an automated electron diffraction pattern indexing tool attached to the TEM (ACOM-TEM) of the Al 7075-O alloy after two ECAP processing paths, 3p-130 °C and 8p-130 °C.

important change observed with increasing N_p or decreasing T_p, i.e. processing severity, was the decrease of both the width and the length of the (sub)grains, rapidly for the initial strains (one pass), and more slowly at higher severity degrees (Tables 2 and 3). Accordingly, similar (sub)grain size (~150 nm) has been achieved after the most severe processing paths, i.e. 3p-80 °C and 8p-130 °C (Fig. 2d and e).

Another feature revealed in the TEM micrographs of Fig. 2 is a large number of fine bright particles distributed through the grains, which have been indicated by black arrows. These spherical precipitates coarsened during the previous overaging treatment but remained unaffected by ECAP processing, with sizes similar to the initial overaged state, ranging from ~100 to ~200 nm.

Fig. 3 shows grain-boundary misorientation distributions corresponding to Al 7075-O alloy samples subjected to 3 and 8 ECAP passes at 130 °C. These misorientation distributions have been obtained by an automated electron diffraction pattern indexing tool attached to the TEM (ACOM-TEM). After a strain of $\varepsilon \sim 3$ (3 passes) many low misorientation and few high misorientation boundaries are observed. The fraction of high-angle grain boundaries (f_{HAB}) after 3 passes was 37%. After eight passes ($\varepsilon \sim 8$), the grain boundary spacing was further decreased and eventually a more uniform, finer grain structure developed which was aligned with the shear direction of the last pass (Fig. 2d). These lamellar boundaries were predominantly high-angle in character and contained few transverse LAGBs, and thus, f_{HAB} has been increased up to 56% after 8 passes.

Fig. 4 shows tensile curves of the engineering stress versus plastic elongation (s–e curve) at room temperature for the as start Al 7075-O alloy, and after different ECAP processing conditions. Fig. 4a includes curves after ECAP processing through one pass at room temperature, and curves corresponding to samples tested as a function of the number of ECAP passes at 130 °C. On the other hand, Fig. 4b shows tensile curves for samples tested after ECAP processing by 3 passes at different temperatures.

Additionally, values corresponding to different parameters extracted from the tensile curves for all processed samples have been included in Table 3: the yield stress ($s_{0.2}$) given by the stress at 0.2% plastic elongation; the maximum stress (s_{max}) of the tensile curve; the uniform plastic elongation (e_u) defined by the plastic elongation at the maximum stress; and the plastic elongation at fracture (e_F).

The tensile curve corresponding to the as start Al 7075-O alloy showed nearly steady state, which indicated that it performed a large amount of substantially uniform elongation [31]. The as start
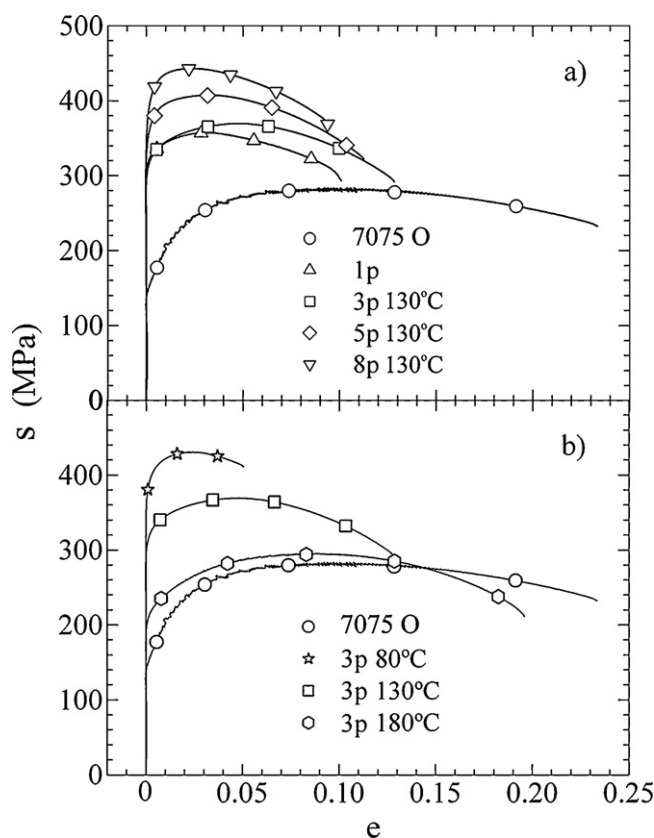

Fig. 4. Engineering stress vs. plastic elongation (s–e curves) obtained by tensile tests of the as start Al 7075-O alloy and after ECAP processing: (a) as a function of the number of passes at 130 °C; (b) as a function of the processing temperature and three ECAP passes.

Al 7075-O alloy is very ductile in its overaged and coarse-grained form. It has an elongation to failure as large as 26% (Table 3), but low yield strength (155 MPa).

The strength of the ECAPed materials differs depending on the processing conditions, i.e. number of passes and processing temperature. After one pass at room temperature a rapid increase in the yield stress value (325 MPa) and maximum tensile strength (357 MPa) (see Table 3) was observed, being approximately twice higher than those for the coarse-grained as start Al 7075-O alloy. The elongation of the 1p-ECAPed Al 7075-O alloy is, however, lower. The uniform elongation is only 3.1% and the total elongation is 10%.

A comparison of the stress–elongation curves of the 1p-ECAP sample and the samples processed by higher number of passes, 3–8 passes at 130 °C, is presented in Fig. 4a. Both the yield stress ($s_{0.2}$) and the maximum stress (s_{max}) increase with increasing number of passes (N_p) until a maximum value of 399 and 442 MPa, respectively, after 8 ECAP passes at 130 °C. However, the elongation to failure remains almost unaltered after the large decrease after the first pressing at room temperature (Fig. 4a and Table 3). Thus, there is an important strength increase with little change in elongation when processing at 130 °C for 5 or 8 ECAP passes.

Likewise, uniform elongation, which represents the maximum practical elongation in engineering application before instability in tension, was significantly reduced after one ECAP pass at room temperature, from 9.8% for the as start Al 7075-O alloy to 3.1% for ECAP-1p T_{RT}. However, the increase in number of passes produces similar uniform elongation values than that after 1p-T_{RT}, while the yield strength is considerably improved (Table 3). This is in contrast to the expected behaviour after increased severe plastic deformation, where an increase in strength together with a decrease in elongation would be expected. On the other hand, for the same

number of ECAP pressings ($\varepsilon \sim 3$) (Fig. 4b), a processing temperature of 80 °C led to high values of yield strength (392 MPa) with low values of uniform and total elongation (see also Table 3). Also shown here is the decrease in strength and increase in elongation after ECAP processing at the higher temperature of 180 °C due to the presence of larger grains (Fig. 2f), which were recovered and partially recrystallized during the processing at higher temperature. Thus, the lower the ECAP processing temperature, the higher the maximum stress and the lower the material elongation.

4. Discussion

This work is focused in the effect of ECAP processing variables, such as the number of passes (N_p) and processing temperature (T_p), which determine the processing severity, on the mechanical properties at room temperature of an Al 7075-O alloy. Additionally, in this section, the correlation between the microstructural evolution and the mechanical properties at room temperature of the ultra-fine grained Al 7075-O alloy processed by ECAP will be discussed.

The Al 7075 alloy was overaged at 280 °C during 5 h previously to ECAP processing to facilitate the ECAP deformation and to introduce larger accumulative strains than it would be possible in the as-received T6 temper. Thus, the coarsened precipitates present in the overaged alloy have less effect on the mechanical properties, because they remain coarser and more separated than in the T6 state. However, the higher refining of the ECAPed Al 7075-O, respect to pure aluminium, is due to the presence of these particles, 100–200 nm in size. Thus, it is our contention that the major strengthening factors will be on one side the high density of dislocations retained inside the grains, especially after the first passes of deformation or at low processing temperatures, and on the other side the grain refinement strengthening by the Hall–Petch effect, related to the interaction between dislocations and grain boundaries.

Fig. 2 and Table 3 shows the (sub)grain size data for all processing conditions. After ECAP processing, the elongated pancake-shaped grains in the as start material changed to fine elongated (sub)grains in the shear direction of the last pass (Fig. 2).

It can be observed from Figs. 2 and 3 that these structures were constituted by cell walls with very low misorientations, although the fraction of high-angle grain boundaries (f_{HAB}) increases with N_p from ~37% after 3 ECAP passes to ~56% after 8p. The relatively high fraction of LABs even at $\varepsilon \sim 8.0$ ($N_p = 8$) is a characteristic of a deformation induced microstructure, where transient LABs are being continuously formed during strain, and low and medium angle boundaries are always present [32–37]. When the ECAP processing was carried out at higher temperature (180 °C), dislocation recovery was favoured, producing coarser grains as illustrated in Fig. 3f.

It is worth to note that the microstructure obtained after ECAP processing of the Al 7075-O is determined mainly by the severity of deformation. This parameter is properly characterized by the maximum force (F_{max}) reached during the last pass of each ECAP path considered (Table 2). Furthermore in Table 2, it has been shown that F_{max}, i.e. the degree of severity during the ECAP path, increases with N_p and decreases with T_p, being very similar for the ECAP paths consisting of 3p-80 °C and 8p-130 °C. Thus both processing paths suggest analogous severity levels, leading to similar (sub)grain size (~150 nm).

On the other hand, if the processing severity determines microstructure, likewise it will determine largely the mechanical properties of the ECAP processed materials. Accordingly, Fig. 5 shows the relationship between the yield stress ($s_{0.2}$) and the uniform plastic elongation (e_u) as a function of F_{max}, for all ECAP
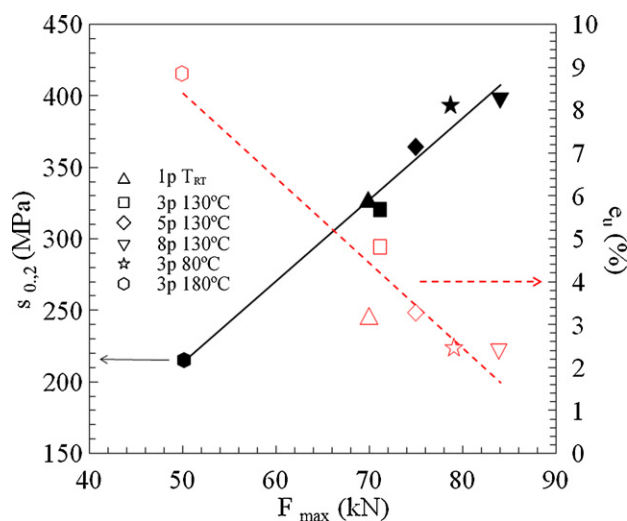

Fig. 5. Yield stress ($s_{0.2}$) (solid symbols) and uniform plastic elongation (e_u) (open symbols) obtained by tensile tests against the processing severity (F_{max}). The maximum load (F_{max}) recorded during the last pass of each ECAP processing considered in this study is an appropriate estimation of the processing severity. The regression lines for the correlation between $s_{0.2}$ vs. F_{max} and e_u vs. F_{max} have been represented by a solid line (black) and dashed line (red) respectively. (For interpretation of the references to color in this figure legend, the reader is referred to the web version of the article.)

processing conditions considered. For both mechanical parameters, $s_{0.2}$ and e_u, a linear relationship with the processing severity can be observed (F_{max}), being an inverse relationship for e_u and direct for $s_{0.2}$. Accordingly, a maximum value of $s_{0.2}$ after 3p-80 °C and 8p-130 °C is observed, which correspond to the most severe conditions considered in this study. On the opposite, the lowest $s_{0.2}$ value is obtained after ECAP processing after 3p at 180 °C, which shows the lowest severity or F_{max} value, and the largest (sub)grain size (Fig. 3f). However, it seems from Fig. 5 that for a wide interval of high F_{max} values (70–84 kN), similar e_u values are obtained. Thus, the yield stress increases clearly with the processing severity, because the severity determines the stress withstood by the sample, and therefore the subgrain size achieved. However, the relationship between the uniform elongation with the processing severity is not so precise, because other microstructural parameters such as the grain boundary misorientation or the dislocation density can be involved.

Fig. 6 shows the relationship between the yield stress and total elongation for the as start Al 7075-O alloy after ECAP with various processing conditions. ECAPed Al 7075-O alloy follows a general trend such that yield stress is inversely proportional to tensile elongation. This implies that as the material is strengthened, it becomes less ductile. These data for the current ECAPed Al 7075-O alloy are in agreement with previous results obtained by other researchers on ECAPed aluminium alloys, after various heat treatment conditions [38,39]. Both strength and ductility are related to the microstructure developed, because of the accumulation of plastic deformation during the ECAP processing and the amount of prior work hardening that has been imposed.

However, Fig. 6 confirm a notable increase in yield strength with similar elongation to failure on ECAP processed material by 8 passes at 130 °C respect to 1p at room temperature. It is our contention that mobile dislocation density is reduced by recovery after processing at 130 °C (Fig. 2). The reduced dislocation density can produce lower strength levels, but this is compensated by grain refining produced by an increase in the number of passes, being responsible for delaying strain localization and fracture. Such delayed failure at the processing temperature of 130 °C is particularly remarkable in comparison with ECAPed material at 80 °C, which failed practi-
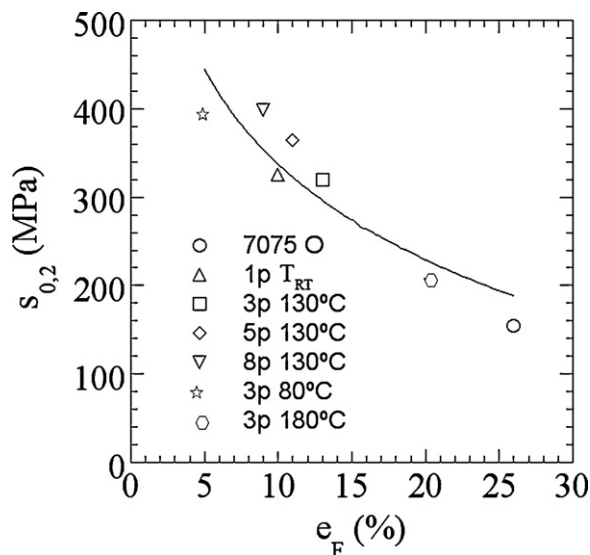
Fig. 6. Yield stress ($s_{0.2}$) vs. plastic elongation at fracture (e_F) obtained by tensile tests of the as start Al 7075-O alloy and after ECAP processing.

Fig. 7. Yield stress ($s_{0.2}$) vs. (sub)grain size (L_Y) for the Al 7075-O alloy after ECAP processing. The regression lines for the correlation between $s_{0.2}$ vs. L_Y^{-1} and $s_{0.2}$ vs. $L_Y^{-1/2}$ have been represented by a solid line and a dashed line respectively.

cally at the maximum tensile strength (Figs. 4 and 6). Thus, it is our contention that although the processing severity was similar for both processing conditions (Table 2), however, the lower temperature for the processing 3p-80 °C limits dislocation recovery during processing, decreasing the elongation at fracture.

On the other hand, it is expected that the improvement in mechanical strength after ECAP processing will be related to the (sub)grain refining achieved according to the following equation:

$$s_y = s_0 + kL^{-q} \tag{1}$$

where q is the (sub)grain size exponent and has values ranged between 0.5 and 1.

For materials with fine grain size and mainly high angle grain boundaries (HABs), q is equal to 0.5, and Eq. (1) corresponds to the Hall–Petch relationship. On the other hand, materials subjected to cold deformation present a microstructure consisting of a mixture of grains and (sub)grains with high density of dislocations and low angle grain boundaries (LABs). For these materials, q will be ~1. Thus, the strengthening due to dislocation walls and LABs can be described as a L^{-1} dependence, instead of the $L^{-1/2}$ dependence expected for high angle grain boundaries [40].

To determine the relationship between the strength and the grain size (L_Y) of the ECAPed Al 7075-O alloy samples, in Fig. 7 the yield stress has been represented against L_Y^{-1} (solid line) and against $L_Y^{-1/2}$ (dashed line) for all ECAP conditions considered in the present work.

Both set of points, $s_{0.2} - L_Y^{-1}$ and $s_{0.2} - L_Y^{-1/2}$, fit to straight lines, whose corresponding equations also have been included in the graph. At first sight, the two equations can look correct, however the relationship $s_{0.2} - L_Y^{-1/2}$ (dashed line) leads to a negative value of s_0 and a slope $k = 241$ MPa μm$^{1/2}$, which is five times higher than the Hall–Petch slope for pure aluminium (40–60 MPa μm$^{1/2}$) [41]. However, the fit for the relationship $s_{0.2} - L_Y^{-1}$ shows close values of k and s_0 to those obtained by a similar fit for pure aluminium processed by cold deformation. On the other hand, the value of the k constant normalized by Gb, where G is the shear modulus and b is the modulus of the Burgers vector, is ~7. This value is very close to those currently obtained for a large number of alloys [42]. Therefore, it is our contention that the improvement in mechanical strength after ECAP processing for the Al 7075-O correlates better with the presence of a (sub)grain microstructure (LABs) and high
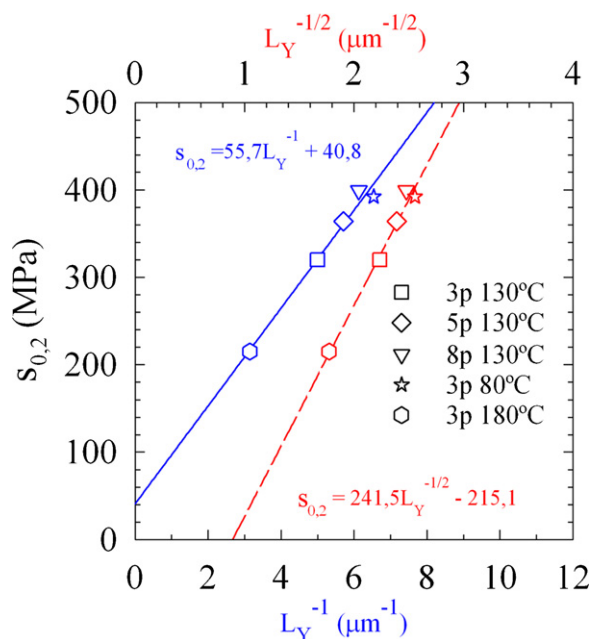
dislocation density than with a very fine grain size (HABs). Thus, a linear dependence between stress and L_Y^{-1} is obtained.

On the other hand, the ductility decrease after certain conditions of ECAP processing is in agreement with previous results of materials processed by SPD techniques. According to Considere's plastic stability criterion (Eq. (2)) [43,44], the uniform plastic deformation depends on the work hardening ability of the tested material as:

$$\left(\frac{\partial \sigma}{\partial \varepsilon}\right)_{\dot{\varepsilon}} \le \sigma \tag{2}$$

where σ and ε are true stress and true strain, respectively. The nanocrystalline and ultrafine matrix grains tend to lose the work hardening ability (left-hand side of Eq. (2)) quickly on deformation owing to their very low dislocation storage efficiency inside the tiny grains [45]. Such a high-strength material is therefore prone to plastic instability (early necking), severely limiting the desirable uniform elongation.

Accordingly, in Fig. 8 it has been represented $s_{max} - s_{0.2}$ against uniform plastic elongation (e_u). $s_{max} - s_{0.2}$ has been considered as a good estimation of the work hardening capacity, since raw data are taken into account, and it is avoided the uncertainty involved in calculating the work hardening exponent, N. A linear relationship between $s_{max} - s_{0.2}$ and the resulting uniform elongation is observed. In general, the 7075-O alloy processed by most of the ECAP processing conditions considered in this study exhibits little work hardening, and as a result, the stress peak is quickly formed at very low strains. This result occurs because the dislocation density in ultrafine-grain sample saturates due to the annihilation of dislocations into the grain boundaries. When the grain size is reduced to the nanocrystalline regime, the mean free path of dislocations generated at grain-boundary sources is severely limited. Rather than cross slipping and generating work hardening, these dislocations can run freely until they meet the opposing grain boundary, which acts as a sink. Thus, the dislocation density remains low throughout the plastic deformation process, and work hardening is not significant [46].

Accordingly, further increase in uniform and total elongation after ECAP processing at high processing temperature (3p-180 °C)
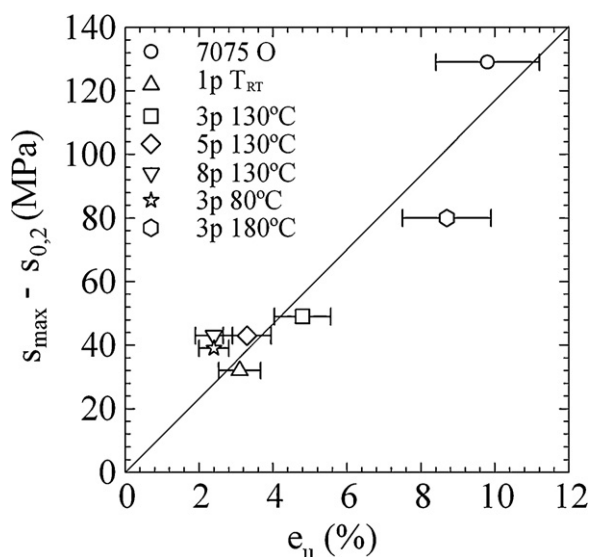
Fig. 8. . $s_{max} - s_{0.2}$ vs. uniform plastic elongation (e_u) obtained by tensile tests of the as start Al 7075-O alloy and after different conditions of ECAP processing.

or by low number of passes (3 passes at 130 °C) is thought to have been determined by dislocation-density reduction. Thus, work hardening will be improved during the tensile test as dislocation density is reduced due to a less severe ECAP processing. Accordingly, processing at higher temperature (180 °C) caused grain growth (Fig. 2f) and larger uniform elongation and work hardening, but with a large decrease in strength as shown in Fig. 4. On the contrary, the low work hardening rate of the alloy processed by 1 ECAP passes at RT may imply a difficulty of storing additional dislocations, causing localized deformation and leading to low ductility (Fig. 4). Additionally, processing by 3–5 passes at 130 °C also shows obvious work hardening ability (Fig. 8), favouring the plastic stability and the increase in strength until the UTS during the tensile test (Fig. 4a and Table 3), unlike most UFG/nanocrystalline metals and alloys that reach the tensile curves peak very early with small plastic deformation [47].

Finally, the ECAPed samples processed at 130 °C and different number of passes exhibit similar values of strain hardening (Fig. 8), with improved values of the ultimate tensile strength with increasing N_p, and without significant loss in uniform and total elongation (Fig. 4a and Table 3). It is our contention, that $T_p = 130$ °C favours some recovery during processing and an increase in the fraction of high-angle boundaries with increasing N_p, being $f_{HAB} = 37\%$ after 3p and $f_{HAB} = 56\%$ after 8p (Fig. 3). Accordingly, the increase in N_p allows sustaining similar ductility together with higher tensile strength for the sample processed by 8 ECAP passes at 130 °C.

In summary, the results from these experiments demonstrate that successful processing may be undertaken up to eight ECAP passes by conducting the pressing operation in samples in an overaged-as-start state. Furthermore, control of processing variables, N_p and T_p, allows optimizing strength and ductility.

5. Conclusions

The tensile properties at room temperature of overaged Al 7075-O alloy processed by ECAP were analyzed. ECAP processing was performed using route B_C at different temperatures and number of passes, which determine the processing severity. The main conclusions of this study are as follows:

The microstructure and the yield stress obtained after ECAP processing is determined mainly by the processing severity. After the most severe conditions of ECAP processing, i.e. 8p-130 °C and

3p-80 °C, the (sub)grain size was reduced down to ~150 nm. Consequently, tensile testing at room temperature revealed a significant increase in yield and maximum tensile strength with respect to the as start material.

The highest maximum stress value was 442 MPa, corresponding to ECAPed Al 7075-O sample by 8 passes at 130 °C.

As the number of ECAP passes at 130 °C increases from 3 to 8 passes, a marked improvement in yield and maximum tensile strength was found without significant loss of elongation respect to the first ECAP pass at room temperature. This is due to an increase in f_{HAB} and a decrease of intragranular dislocation density with increasing N_p.

Although the processing severity was similar for 3p-80 °C and 8p-130 °C, the lower T_p for the ECAP path 3p-80 °C limits dislocation recovery during processing, decreasing the elongation at fracture.

Severe plastic deformation at higher temperature (180 °C) decreases the processing severity and leads to coarser grain size. As a result, lower mechanical strength and higher elongation was obtained.

After processing by one ECAP pass at room temperature the marked decrease in ductility respect to the as start material is due to the loss of work-hardening ability, and the high density of accumulated dislocations.

The improvement in mechanical strength at room temperature after ECAP processing is mainly correlated to strengthening due to (sub)grain microstructure and low angle grain boundaries (LABs).

References

[1] H.T. Lee, G.H. Shaue, Mater. Sci. Eng. A268 (1999) 154–164.
[2] J.M. García-Infanta, A.P. Zhilyaev, A. Sharafutdinov, O.A. Ruano, F. Carreño, J. Alloy Compd. 473 (2009) 163–166.
[3] C.M. Cepeda-Jiménez, J.M. García-Infanta, M. Pozuelo, O.A. Ruano, F. Carreño, Scripta Mater. 61 (2009) 407–410.
[4] R. Jayaganthan, H.-G. Brokmeier, S.K. Bernd Schwebke, Panigrahi, J. Alloy Compd. 496 (2010) 183–188.
[5] C.M. Cepeda-Jiménez, J.M. García-Infanta, A.P. Zhilyaev, O.A. Ruano, F. Carreño, J. Alloy Compd. 509 (2011) 636–643.
[6] C.C. Koch, Scripta Mater. 49 (2003) 657–662.
[7] R. Islamgaliev, N. Yunusova, I. Sabirov, A. Sergueeva, R.Z. Valiev, Mater. Sci. Eng. A 319–321 (2001) 877–881.
[8] Y. Wang, M. Chen, F. Zhou, E. Ma, Nature 419 (2002) 912–915.
[9] R.Z. Valiev, Adv. Eng. Mater. 5 (2003) 296–300.
[10] E. Ma, Scripta Mater. 49 (2003) 663–668.
[11] Z. Budrovic, H. Van Swygenhoven, P.M. Derlet, S. Van Petegem, B. Schmitt, Science 304 (2004) 273–276.
[12] M. Dao, L. Lu, R.J. Asaro, J.T.M. De Hosson, E. Ma, Acta Mater. 55 (2007) 4041–4065.
[13] J.M. García-Infanta, A.P. Zhilyaev, C.M. Cepeda-Jiménez, O.A. Ruano, F. Carreño, Scripta Mater. 58 (2008) 138–141.
[14] T. Grosdidier, D. Goran, G. Ji, N. Llorca, J. Alloy Compd. 504S (2010) S456–S459.
[15] Y. Iwahashi, Z. Horita, M. Nemoto, T.G. Langdon, Acta Mater. 45 (1997) 4733–4741.
[16] R.S. Mishra, R.Z. Valiev, S.X. McFadden, A.K. Mukherjee, Mater. Sci. 252 (1998) 174–178.
[17] M. Furukawa, Y. Ma, Z. Horita, M. Nemoto, R.Z. Valiev, T.G. Langdon, Mater. Sci. Eng. A 241 (1998) 122–128.
[18] R.Z. Valiev, R.K. Islamgaliev, I.V. Alexandrov, Prog. Mater. Sci. 45 (2000) 103–189.
[19] A. Gholina, P.B. Prangnell, M.V. Markushev, Acta Mater. 48 (2000) 1115–1130.
[20] S.D. Terhune, D.L. Swisher, K. Oh-Ishi, Z. Horita, T.G. Langdon, T.R. McNelley, Metall. Mater. Trans. A 33 (2002) 2173–2184.
[21] N.Q. Chinh, J. Gubicza, T. Czeppe, J. Lendvai, C. Xu, R.Z. Valiev, T.G. Langdon, Mater. Sci. Eng. A 516 (2009) 248–252.
[22] Z.C. Duan, N.Q. Chinh, C. Xu, T.G. Langdon, Metall. Mater. Trans. A 41 (2010) 802–809.
[23] Y.H. Zhao, X.Z. Liao, Z. Jin, R.Z. Valiev, Y.T. Zhu, Acta Mater. 52 (2004) 4589–4599.

[24] Y.H. Zhao, X.Z. Liao, Y.T. Zhu, R.Z. Valiev, J. Mater. Res. 20 (2005) 288–291.
[25] S. Lee, A. Utsunomiya, H. Akamatsu, K. Neishi, M. Furukawa, Z. Horita, T.G. Langdon, Acta Mater. 50 (2002) 553–564.
[26] C. Xu, M. Furukawa, Z. Horita, T.G. Langdon, Acta Mater. 51 (2003) 6139–6149.
[27] S. Komura, M. Furukawa, Z. Horita, M. Nemoto, T.G. Langdon, Mater. Sci. Eng. A 297 (2001) 111–118.
[28] G. Shigesato, E.F. Rauch, Mater. Sci. Eng. A 462 (2007) 402–406.
[29] E.F. Rauch, M. Veron, Materialwissenschaft und Werkstofftechnick 36 (2005) 552–556.
[30] E.R. Rauch, A. Duft, Mater. Sci. Forum. 495–497 (2005) 197–202.
[31] H.W. Kim, S.B. Kang, N. Tsuji, Y. Minamino, Acta Mater. 53 (2005) 1737– 1749.
[32] C.Y. Yu, P.L. Sun, P.W. Kao, C.P. Chang, Mater. Sci. Eng. A 366 (2004) 310–317.
[33] O. Sitdikov, T. Sakai, A. Goloborodko, H. Miura, R. Kaibyshev, Philos. Mag. 85 (2005) 1159–1175.
[34] C. Kobayashi, T. Sakai, A. Belyakov, H. Miura, Philos. Mag. Lett. 87 (2007) 751–766.
[35] I. Mazurina, T. Sakai, H. Miura, O. Sitdikov, R. Kaibyshev, Mater. Sci. Eng. A 473 (2008) 297–305.
[36] T. Sakai, A. Belyakov, H. Miura, Metall. Mater. Trans. A 39 (2008) 2206–2214.
[37] I. Mazurina, T. Sakai, H. Miura, O. Sitdikov, R. Kaibyshev, Mater. Trans. 50 (2009) 101–110.
[38] S. Ferrasse, V.M. Segal, K.T.H. Hartwig, R.E. Goforth, J. Mater. Res. 12 (1997) 1253–1261.
[39] M. Cai, D.P. Field, G.W. Lorimer, Mater. Sci. Eng. A 373 (2004) 65–71.
[40] J. Weertman, J.R. Weertman, in: R.W. Cahn, P. Haasen (Eds.), Physical Metallurgy, 3rd ed., Holland: Elsevier Science Publishers, Amsterdam, 1983, pp. 1260–1307.
[41] N. Hansen, Acta Metall. 25 (1977) 863–869.
[42] J. Gil Sevillano, P. van Houtte, E. Aernoudt, Prog. Mater. Sci. 25 (1980) 69–412.
[43] E.W. Hart, Acta Metall. 15 (1967) 351–355.
[44] D. Jia, Y.M. Wang, K.T. Ramesh, E. Ma, Y.T. Zhu, R.Z. Valiev, Appl. Phys. Lett. 79 (2001) 611–613.
[45] Y.M. Wang, E. Ma, Mater. Sci. Eng. A 375–377 (2004) 46–52.
[46] M.A. Meyers, A. Mishra, D.J. Benson, Prog. Mater. Sci. 51 (2006) 427–556.
[47] Y.M. Wang, E. Ma, Acta Mater. 52 (2004) 1699–1709.